JOURNAL OF APPLIED ELECTROCHEMISTRY 24 (1994) 66–71

Cathodic codeposition of alloyed materials for use in lithium battery negative electrodes

M. H. CHAPEAU-POINSO, J. BOUTEILLON, J. C. POIGNET

CREM GP/ENSEEG, BP 75 38402 St Martin D'Heres Cedex, France

Received 17 February 1993; revised 29 April 1993

This work aimed at studying the possibility of preparing Wood alloy structures by cathodic codeposition of Bi, Pb, Sn and Cd from aqueous solutions. The metal ions were dissolved in a fluoborate medium. The reduction mechanisms of the single ions, studied using a rotating disc copper electrode or by linear sweep voltammetry, were simple with a single fast electron transfer step, except for the case of Bi, where the reaction was found to be irreversible. By potentiostatic codeposition of the four metals at a copper rotating disc electrode, metallic powders, having a composition close to that of the Wood alloy, with Bi, Sn, Cd and Pb_7Bi_3 phases, were prepared. These powders had homogeneous grains with micrometric sizes, and a specific surface of $1.5\,m^2\,g^{-1}$. Their performances as lithium host structures in negative electrodes will be assessed.

Nomenclature

α	transfer coefficient
k^0	standard rate constant
$E_{i=0}$	thermodynamic potential
$E_p, E_{p/2}$	peak and half-peak potentials
C_{ox}	concentration of the oxidized species at the interface
C^0_{ox}	bulk concentration of the oxidized species
ω	rotation rate (r.p.m.)
i_l	limiting current density
i_p	peak current density
ν	kinematic viscosity

1. Introduction

Room temperature lithium secondary batteries with organic electrolyte, have been developed in recent years [1]. If pure lithium is used as the negative electrode, dendrites are formed on recharging, because of the nature of the electrode kinetics. Furthermore, lithium metal reacts with most organic solvents, creating a passivating layer at the electrode/electrolyte interface [2–5]. One way of avoiding this problem is to replace pure Li with a metallic alloy in which lithium is inserted with a reduced activity. Preliminary studies using Wood alloys (50 mass % Bi, 25 mass % Pb, 12.5 mass % Sn and 12.5 mass % Cd) appeared promising [6–8] because of the high value ($10^{-9}\,cm^2\,s^{-1}$) of the diffusion coefficients for lithium metal in the alloy at room temperature. These studies were performed using an alloy prepared by melting and cooling the relevant mixture of metals, yielding electrodes about 1 cm thick.

However, it appears that studies have stopped due to safety hazards linked to the low melting points of both lithium metal and Wood alloy substrate. Nevertheless, considering the rather high specific capacities [8] and the improved recharging current densities [6], this study is concerned with making Wood alloy structures suitable for battery electrode fabrication, i.e. in the form of thin layers or powders. To obtain these structures, the electrochemical codeposition of the metals, among various other possible techniques such as CVD or plasma deposition, was selected.

The aim of the present work was to study the possibility of making suitable substrates having a composition and microscopic structure close to that of the Wood alloy, by means of cathodic codeposition of the metals. Wood alloy has the following metallic phases: Bi, Pb, Sn, Cd and Pb_7Bi_3.

The standard potentials of the systems in water, vs the standard hydrogen electrode, are: $E^0_{Bi^{3+}/Bi} = 0.215\,V$; $E^0_{Pb^{2+}/Pb} = -0.126\,V$; $E^0_{Sn^{2+}/Sn} = -0.136\,V$; and $E^0_{Cd^{2+}/Cd} = -0.403\,V$.

In the context of cathodic alloy deposition, only Pb–Sn electrochemical deposition has been studied in fluoborate media [9]; the Pb and Sn waves were not discriminated. The reduction of Cd (II) has also recently been studied in the same medium, where hydrogen evolution was shown to be less than in other media [10].

2. Experimental conditions

2.1. *Solvent and electrolytes*

Aqueous solutions of HBF_4 0.47 M + H_3BO_3 0.2 M (pH 0.8) were selected [11]. Here the role of H_3BO_3

0021-891X

is to hinder the formation of HF:

$$HBF_4 \Longrightarrow H^+ + BF_4^-$$

$$BF_4^- \Longleftrightarrow BF_3 + F^-$$

$$BF_3 + 3H_2O \Longleftrightarrow H_3BO_3 + 3HF$$

The overall hydrolysis reaction can be written:

$$HBF_4 + 3H_2O \Longleftrightarrow H_3BO_3 + 4HF$$

The value of the ratio $[HBF_4]/[H_3BO_3]$ was selected as indicated so that the reaction above is shifted to the left, thus avoiding HF formation and possible precipitation of metal fluorides such as PbF_2 and SnF_2. The metals were introduced as oxides: Bi_2O_3, PbO, SnO and CdO. All the chemical products used were Prolabo 'Normapur'.

2.2. *Cell, electrodes and electrical device*

A Plexiglas cell was used with a 3-electrode system. The working electrode was made of copper, a metal which does not reduce spontaneously the metal ions studied, and because hydrogen evolution on copper is rather slow. When necessary, for some specific anodic studies, a vitreous carbon electrode was also used. These 1 cm thick disc electrodes were either motionless or rotated (Tacussel ED1 101 T system), and had a surface of $0.78\,cm^2$. The discs were embedded in Teflon. The reference electrode was a KCl-saturated calomel electrode. The auxiliary electrode was a graphite cylinder.

Prior to each experiment, the copper electrodes were mechanically polished then dipped into a dilute solution of nitric acid and rinsed with pure water. Argon was bubbled through the solution for 30 min before the experiment started, and bubbling was maintained over the solution during the whole experiment. A PAR 273 potentiostat-galvanostat was used, and the data were recorded using a Nicolet 4094C digital scope, then processed by a HP 300 computer.

3. Results

3.1. *Reduction of single ions: voltammetric and rotating disc determinations*

Typical linear sweep voltammograms, such as those in Fig. 1, show that for each metallic couple the reductions occurred via a single step, and yielded a product of constant activity. The reaction products obtained by potentiostatic electrolysis and analysed by X-ray diffraction were pure Bi, Pb, Sn and Cd. During the return sweep, the re-oxidation stripping peak of the metal produced was observed, except for the case of bismuth, because the oxidation of the copper electrode interfered. The bismuth re-oxidation stripping peak was, in such cases, demonstrated using a vitreous carbon electrode (Fig. 2). The cadmium reduction peak was obviously distorted by hydrogen evolution. The current density due to hydrogen was estimated using a cadmium electrode in a cadmium-free solution: in the potential domain studied, the hydrogen current density, starting from −0.8 V vs SCE, remained less than $0.5\,mA\,cm^{-2}$.

The peak current densities were proportional to the square root of the sweep rate for sweep rates between $5\,mV\,s^{-1}$ and $100\,mV\,s^{-1}$, as shown in Fig. 3. In the case of cadmium, the current density was corrected for the hydrogen current density. Therefore mass transfer was diffusion controlled.

The rapidity of the electron transfer steps was estimated using the $E_p - E_{p/2}$ criterion. The corresponding values, extrapolated to zero sweep rate for ohmic drop correction, are reported in Table 1.

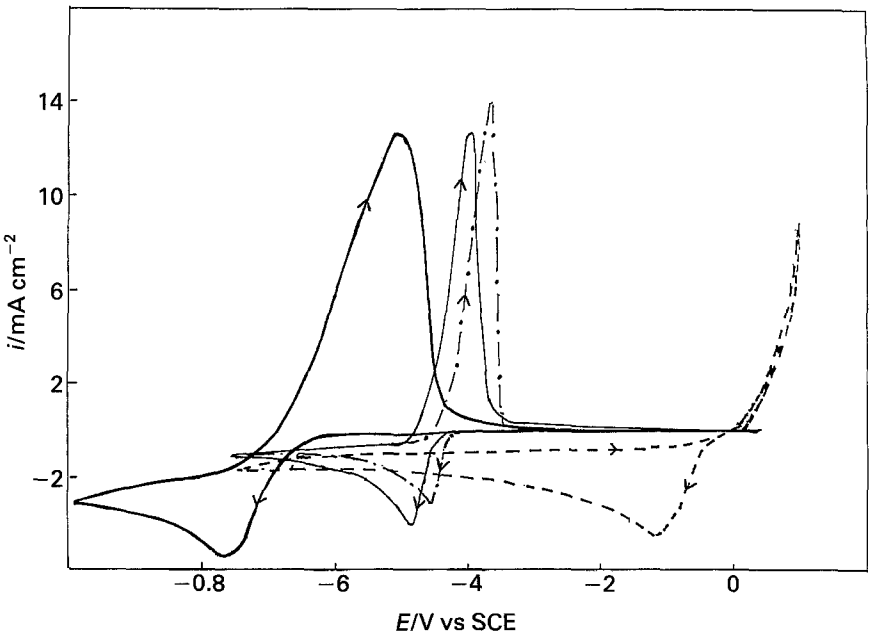

Fig. 1. Voltammograms of a motionless copper electrode in a HBF_4–H_3BO_3 solution. Legend: (– – –) [Bi (III)] = 7.86×10^{-3} M; (– · – · –) [Pb (II)] = 4.57×10^{-3} M; (——) [Sn (II)] = 6.18×10^{-3} M; (——) [Cd (II)] = 2.64×10^{-2} M.

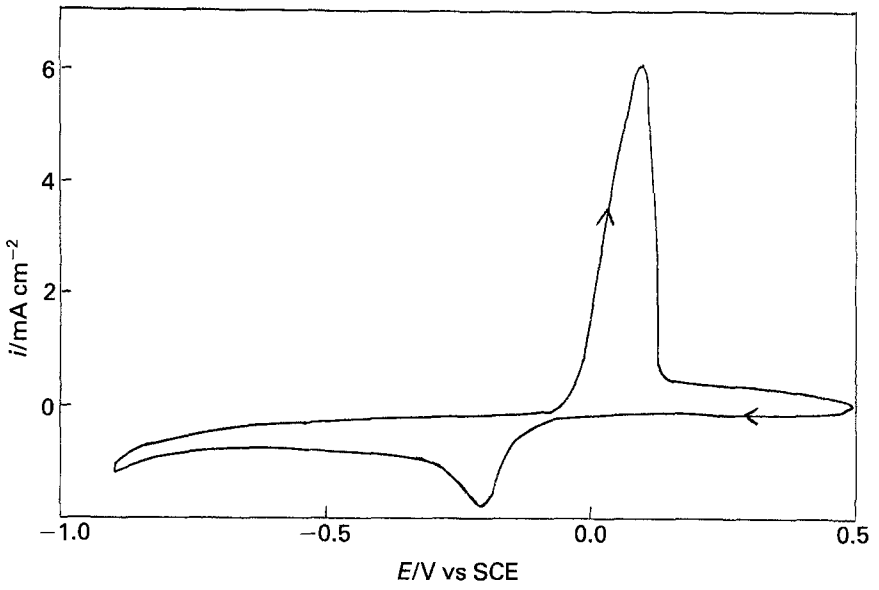

Fig. 2. Voltammogram of a motionless vitreous carbon electrode in a solution of HBF_4–H_3BO_3 containing 5.8×10^{-3} M [Bi (III)].

The theoretical relation: $E_p - E_{p/2} = -0.77\,RT/nF$, for reversible reactions with an insoluble product [12] have been reported in Table 1 with $n = 3$ for Bi, and $n = 2$ for Pb, Sn, and Cd. The results show that, in the case of the divalent metals, the reactions can be considered as reversible. This is not the case for Bi, where the reaction must be considered as irreversible. In fact, the hypothesis of a quasireversible reaction for Bi (III) reduction must be discarded because i_p is proportional to the square root of the sweep rate [13].

The steady state curves obtained at a copper rotating disc electrode, for rotation speeds from 500 to 2000 r.p.m. and a sweep rate of $100\,mV\,s^{-1}$ again show that the reduction of the metal ions occurs via a single step with a limiting diffusion current, as shown in Fig. 4 for the case of lead. The diffusion plateau was imperfect in the case of cadmium because of interference by hydrogen evolution. Re-oxidation peaks were found in the case of Cd, Sn and Pb, but not in the case of bismuth because of copper oxidation. The Levich law was obeyed (Fig. 5), since the variations of the limiting current density i_l were proportional to the square root of the rotation speed, in the case of bismuth, lead and tin, for rotation speeds between 500 and 2000 r.p.m. From the slope of these curves, the diffusion coefficients were calculated:

$$i_l = nFD^{2/3}\omega^{1/2}\nu^{-1/6}C \qquad (1)$$

The results, checked by chronopotentiometric determinations, are:

$$D_{Bi(III)} = (5.6 \pm 0.7) \times 10^{-6}\,cm^2\,s^{-1}$$

$$D_{Pb(II)} = (1.5 \pm 0.05) \times 10^{-5}\,cm^2\,s^{-1}$$

$$D_{Sn(II)} = (5.0 \pm 0.07) \times 10^{-6}\,cm^2\,s^{-1}$$

$$D_{Cd(II)} = (1.4 \pm 0.04) \times 10^{-6}\,cm^2\,s^{-1}$$

(chronopotentiometric evaluation only)

For a given rotation speed, the plots of i_l against C^0_{ox} were also linear (Fig. 6), in agreement with the Levich law.

In the case of bismuth, considering that the reaction was irreversible and gave an insoluble product, the logarithmic analysis (Equation 4) of the i–E steady state curves was made. The Butler–Volmer law:

$$i = nFk^0C_{ox}\exp[-\alpha nF(E - E_{i=0})/(RT)] \qquad (2)$$

yielded, with $C_{ox} = C^0_{ox}(1 - i/i_l)$

$$i = nFk^0C^0_{ox}(1 - i/i_l)\exp[-\alpha nF(E - E_{i=0})/RT] \qquad (3)$$

hence

$$\log[i \times i_l/(i - i_l)] = \log nFk^0 + \log C^0_{ox} - 2.3\alpha nF(E - E_{i=0})/RT \qquad (4)$$

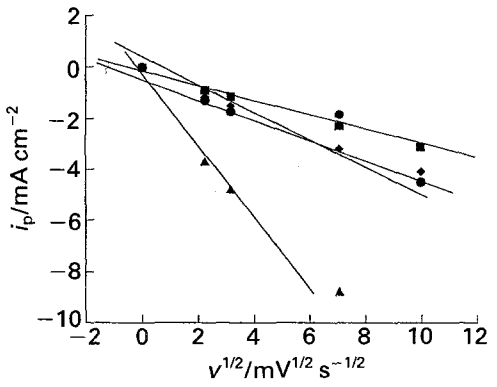

Fig. 3. Plots of cathodic peak current densities vs the square root of scan rate (●) Bi, (■) Pb, (◆) Sn and (▲) Cd.

Table 1. Experimental values of $E_p - E_{p/2}$, with the corresponding theoretical values for rapid reactions

Element	*Bi (III)*	*Pb (II)*	*Sn (II)*	*Cd (II)*
$E_p - E_{p/2}$/mV	−24	−10	−9	−14
$-0.77\,RT/nF$	−6.6	−9.9		

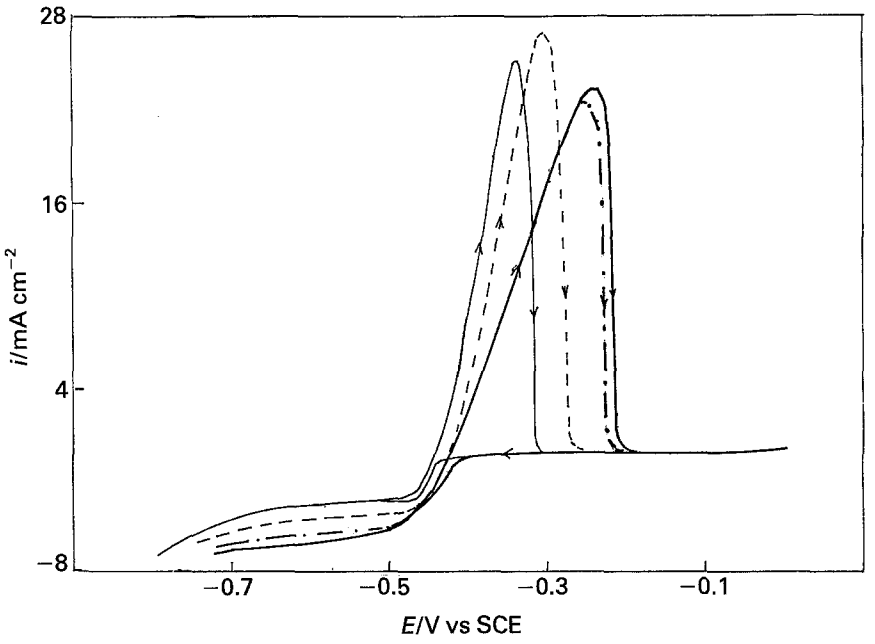

Fig. 4. Current density against voltage curves for different rotation rates on a rotating copper disk electrode in a HBF_4–H_3BO_3 solution containing 4.57×10^{-3} M [Pb (II)], Scan rate: 100 mV s^{-1}. Rotation rates: (——) 500; (– · – ·) 1000; (– – –) 1500; and (——) 2000 r.p.m.

The variations of $\log [i \times i_l/(i - i_l)]$ against E were linear. From the slope and intercept of the straight line obtained (Fig. 7) the kinetical parameters were determined for Bi(III) ion reduction: $\alpha = 0.16$ (assuming $n = 3$) and $k^0 = 2 \times 10^{-3}$ cm s^{-1}.

The logarithmic treatment of the steady state curves yielded standard potentials very close to those of the non-complexed metal ions. Therefore, these metal ions can be considered as non complexed by the BF_4^- ions.

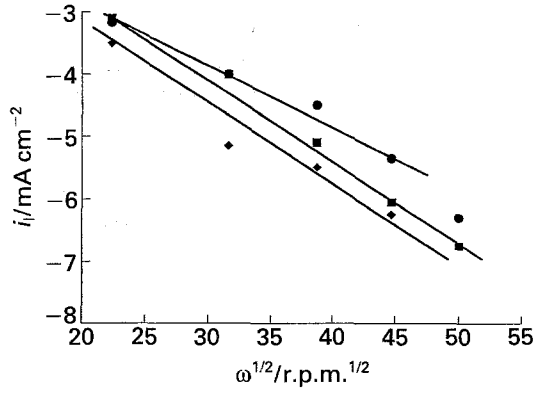

Fig. 5. Plots of the limiting current density against the square root of the rotation rate (●) Bi, (■) Pb and (◆) Sn.

3.2. *Coreduction of the four metal ions: voltammetric and rotating disc electrode studies*

One of the objectives being to obtain a material having a composition close to that of the Wood alloy (50 mass % Bi, 25 mass % Pb, 12.5 mass % Sn and Cd), the composition of the solution was determined assuming that the partial reduction currents, for a potentiostatic step at a potential value of −0.75 V vs SCE, would be equal to the limiting currents observed during the single ion reduction experiments. This procedure yielded the following composition:

$(Bi^{3+}) = 2.85 \times 10^{-3}$ M $\quad (Pb^{2+}) = 1.25 \times 10^{-3}$ M

$(Sn^{2+}) = 1.2 \times 10^{-3}$ M $\quad (Cd^{2+}) = 3.5 \times 10^{-3}$ M

The rotating disc E–i curve ($\omega = 2000$ r.p.m. and $v = 100$ mV s^{-1}) presented in Fig. 8 shows two distinct diffusion plateaux due, respectively, to Bi^{3+}

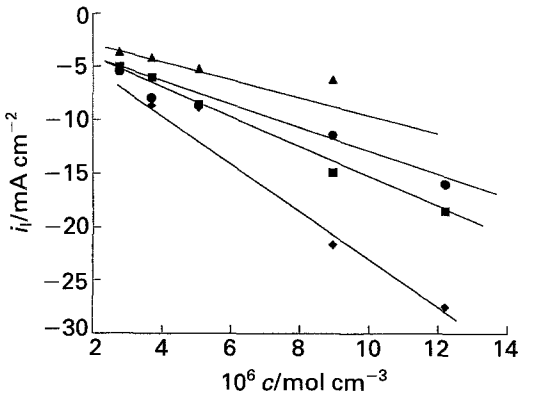

Fig. 6. Plots of the limiting current density against concentration (●) Bi, (■) Pb, (◆) Sn and (▲) Cd.

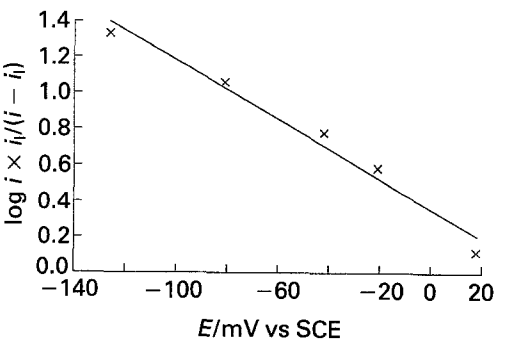

Fig. 7. Plots of $\log (i_l \times i/(i - i_l))$ against potential for Bi (III) reduction.

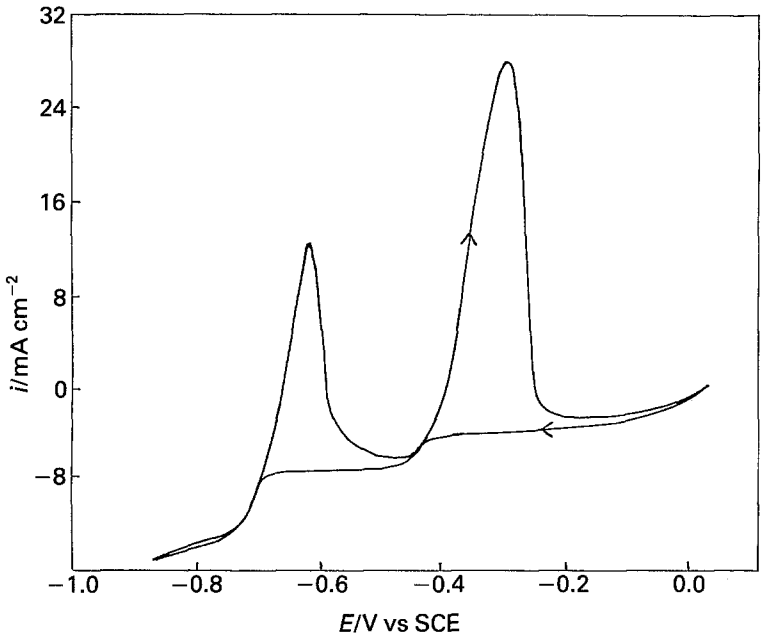

Fig. 8. Current density–voltage curves on a rotating copper disc electrode at a scan rate of 2000 r.p.m. in a HBF_4–H_3BO_3 solution containing 2.85×10^{-3} M Bi^{3+}, 1.25×10^{-3} M Pb^{2+}, 1.2×10^{-3} M Sn^{2+} and 3.5×10^{-3} M Cd^{2+}.

Table 2. Values of $E_{1/2}$ for the four systems in single ion reduction and coreduction experiments

Element	*Bi (III)*	*Pb (II)*	*Sn (II)*	*Cd (II)*
$E_{1/2}$/V (SCE) single ion reduction	−0.1	−0.44	−0.45	−0.75
$E_{1/2}$/V (SCE) coreduction	−0.1	−0.46		−0.70

Table 3. RDE limiting current densities for single ion reductions and for coreduction

Element	*Bi (III)*	*Pb*	*Sn (II)*	*Cd (II)*
i_l/mA cm^{-2} single ion reduction	−5	−2	−1.8	−4
i_l/mA cm^{-2} coreduction	−4	−3.5		−5.5

reduction, then presumably to Sn^{2+} and Pb^{2+} coreduction. The third plateau is ascribable to Cd^{2+} reduction. This curve does not show evidence for any specific interaction between the metals deposited along the direct scan [14, 15]. In fact the $E_{1/2}$ potentials remained practically unchanged from single ion reduction experiments to coreduction experiments, as shown in Table 2. But, on the reverse scans, the characteristics of the bismuth re-oxidation peak depended on the cathodic potential at which the scan was reversed. Figure 9, which was obtained in an electrolyte containing only Bi and Pb ions, shows that when the scan was reversed in the lead deposition potential domain, a first lead reoxidation peak occurred, and the bismuth re-oxidation peak was shifted towards less anodic potentials. In fact, as shown by X-ray diffraction, Pb_7Bi_3 was re-oxidized along this second re-oxidation peak. The formation of this compound probably occurred by a slow chemical reaction between bismuth and lead deposited metals. X-ray diffraction patterns taken a few hours after the deposition experiment showed that this reaction was complete.

The limiting currents were, to a first approximation, equal to the values expectable from the single ion reduction experiments (Table 3).

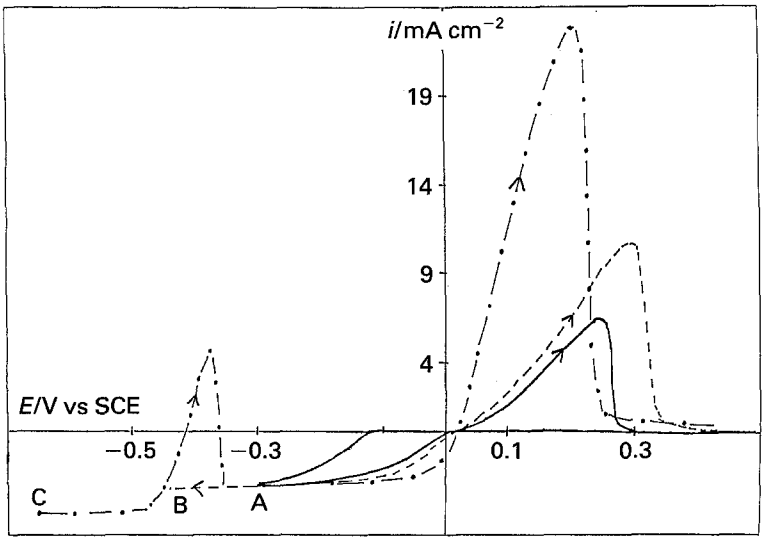

Fig. 9. Current density–voltage curves on a rotating copper disc electrode at a rotation rate of 2000 r.p.m. in a HBF_4–H_3BO_3 solution containing 2.85×10^{-3} M Bi^{3+} and 1.25×10^{-3} M Pb^{2+}. Potential scan: (——) reversed at point A; (– – –) reversed at point B; and (– • – •) reversed at point C.

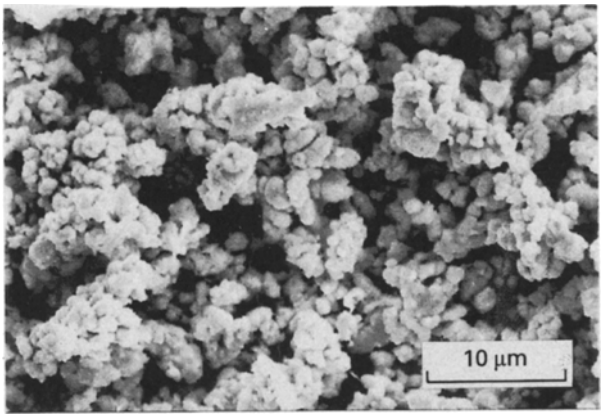

Fig. 10. SEM micrograph of a deposit on copper, potentiostatic mode (−0.75 V vs SCE)

Table 4. Chemical composition of the deposit obtained at $E = -0.75$ V vs SCE, $T = 25°$ C

Element	*Mass %*	*Aimed mass %*
Bi	58	50
Pb	30.6	25
Sn	5.4	12.5
Cd	5.9	12.5

3.3. *Preparation of the codeposited materials*

The deposits were prepared on a copper rotating electrode ($\omega = 2000$ r.p.m.) in a potentiostatic mode at $E = -0.75$ V vs SCE. The deposits obtained were powdery and sufficiently adherent to the electrode to be withdrawn from the solution with the electrode under potentiostatic control. X-ray diffraction analysis showed that the deposit contained pure Bi, Cd, Sn, and Pb_7Bi_3. SEM analysis (Fig. 10) showed that the deposit was made of agglomerates having a diameter about 2 to 3 μm. This deposit was homogeneous from the point of view of its microscopic chemical composition (Fig. 11). The overall compositions of the deposits were analysed by atomic absorption spectroscopy. The characteristic results are presented in Table 4. The overall current efficiency was 90%. The proportions of Bi and Pb were correct, but the Sn and Cd contents were low. Raising the temperature favoured the cadmium contents of the deposit, as shown in Table 5, the proportion of tin in the deposit remaining low. Raising the Sn (II) concentration of the electrolyte resulted in an increase in the tin contents of the deposit (about 7% Sn for a concentration of 2×10^{-3} M).

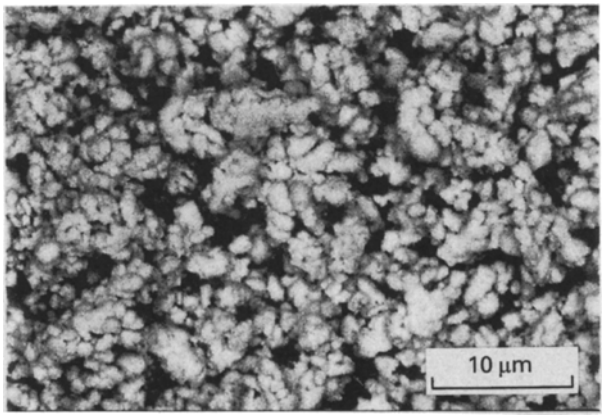

Fig. 11. SEM micrograph of a deposit on copper (backscattered electrons), potentiostatic mode (−0.75V vs SCE)

Table 5. Chemical composition of the deposit obtained at $E = -0.75$ V vs SCE, $T = 50°$ C

Element	*Mass %*	*Aimed mass %*
Bi	55.7	50
Pb	30.0	25
Sn	5.4	12.5
Cd	5.9	12.5

4. Conclusion

The electrochemical deposition of Bi, Pb, Sn and Cd has been studied using linear sweep voltammetry and rotating disc steady state polarisation curves; each solution contained one of the four metallic ions in HBF_4 0.47 M – H_3BO_3 0.2 M solutions. The metallic ions, not complexed in such solutions, were reduced via a single step to the corresponding metals. In all cases the rate was diffusion controlled, and the electron transfer process appeared rapid except for the case of Bi ($\alpha = 0.16$ for $n = 3$, $k^0 = 2 \times 10^{-3}$ cm s^{-1}). The Levich law was obeyed and the diffusion coefficients of the ions were determined. A solution containing the four metal ions in HBF_4–H_3BO_3 was prepared for potentiostatic RDE codepositions of the metals. The deposits obtained were powdery and contained Bi, Cd, Sn and Pb_7Bi_3, with grain sizes of a few micrometres and a specific surface of 1.5 m^2 g^{-1}. These powdery substrates are to be tested as lithium host structures for secondary batteries.

References

[1] Z. Takehara, *J. Power Sources* **26** (1989) 257.
[2] J. G. Thevenin and R. H. Müller, *J. Electrochem. Soc.* **135** (1988) 2422.
[3] R. Herr, *Electrochim. Acta* **35** (1990) 1257.
[4] D. Aurbach, M. L. Daroux, P. W. Faguy and E. Yeager, *J. Electrochem. Soc.* **134** (1987) 1611.
[5] M. Odziemkowski, M. Krell and D. E. Irish, *ibid.* **139** (1992) 3052.
[6] Y. Toyogushi, T. Matsui, J. Yamaura and T. Iijima, *Prog. Batteries & Solar Cells* **6** (1987) 58.
[7] Y. Toyogushi, T. Matsui, J. Yamaura and T. Iijima, *Proc. Electrochem. Soc.* **88** (1988) 659.
[8] M. H. Chapeau-Poinso, Thesis, INP Grenoble (1992).
[9] P. A. Khol, *Plat. Surf. Fin.* **68** (1981) 45.
[10] R. Varma, T. Hoeller, L. Ross and V. S. Agarwala, *J. Electrochem. Soc.* **138** (1991) 162.
[11] A. Brenner, *in* 'Electrodeposition of Alloys,' Academic Press, New York (1963) p. 5.
[12] G. Mamantov, D. L. Manning and J. M. Dale, *J. Electroanal. Chem.* **9** (1965) 253.
[13] H. Matsuda and Y. Ayabe, *Z. Elektrochemie* **59** (1955) 494.
[14] A. R. Despic, V. D. Jovic, R. M. Zejnilovic and J. S. Stevanovic, *J. Appl. Electrochem.* **18** (1988) 511.
[15] A. R. Despic and V. D. Jovic, *J. Electrochem Soc* **134** (1987) 3004.